

Thermodynamic Properties of Superconducting and Non-Superconducting $\text{Pr}_2\text{Ba}_4\text{Cu}_7\text{O}_{15-\delta}$ Compounds with Metallic Double Chains

Takahisa Konno,¹ Michiaki Matsukawa,^{1,*} Keisuke Sugawara,¹ Haruka Taniguchi,¹
Junichi Echigoya,¹ Akiyuki Matsushita,² Makoto Hagiwara,³ Kazuhiro Sano,⁴
Yoshiaki Ohno,⁵ Yuh Yamada,⁵ Takahiko Sasaki,⁶ and Yuichiro Hayasaka⁶

¹*Department of Materials Science and Engineering, Iwate University, Morioka 020-8551, Japan*

²*National Institute for Materials Science, Ibaraki 305-0047*

³*Kyoto Institute of Technology, Kyoto 606-8585, Japan*

⁴*Department of Physics Engineering, Mie University, Tsu 514-8507, Japan*

⁵*Department of Physics, Niigata University, Niigata 950-2181, Japan*

⁶*Institute for Materials Research, Tohoku University, Sendai 980-8577, Japan*

(Dated: December 7, 2015)

To examine the thermodynamic properties of $\text{Pr}_2\text{Ba}_4\text{Cu}_7\text{O}_{15-\delta}$ compounds with metallic CuO double chains, we measured the specific heats of superconducting and non-superconducting polycrystalline samples at low temperatures (1.8–40 K) under various magnetic fields (up to 9 T). In the as-sintered non-superconducting sample, a λ -like enhancement in the specific heat measurement appeared near the antiferromagnetic transition temperature $T_N = 17$ K. In contrast, the reduced superconducting sample with $T_{c,on} = 26.5$ K exhibited no obvious superconducting anomaly in its specific data, but a Schottky-like broad maximum appeared at low temperatures. The Schottky-like anomaly was attributed to low-lying quasi-triplet splitting of Pr^{3+} ions under the crystal field effect.

PACS numbers: 74.25.Ha, 74.25.F-, 74.90.+n

I. INTRODUCTION

Since the discovery of high- T_c copper-oxide superconductors, strongly correlated electron systems have been extensively investigated. Besides the physical properties of two-dimensional CuO_2 planes, researches have focused on the physical role of one-dimensional (1D) CuO chains in some families of high- T_c copper oxides.

Structurally, the Pr-based cuprates, $\text{PrBa}_2\text{Cu}_3\text{O}_{7-\delta}$ (Pr123) and $\text{PrBa}_2\text{Cu}_4\text{O}_8$ (Pr124), are identical to their corresponding Y-based high- T_c superconductors, $\text{YBa}_2\text{Cu}_3\text{O}_{7-\delta}$ (Y123) and $\text{YBa}_2\text{Cu}_4\text{O}_8$ (Y124). Pr123 and Pr124 compounds have insulating CuO_2 planes and are non-superconductive.^{1,2} The suppression of superconductivity in the Pr substitutes has been explained by the hybridization of Pr-4*f* and O-2*p* orbitals.³ The crystal structure of Pr124 with CuO double chains differs from that of Pr123 with CuO single chains. It is well known that CuO single chains in Pr123 and CuO double chains in Pr124 show semiconducting and metallic behaviors, respectively.⁴ The carrier concentration of doped double chains of Pr124 is difficult to vary, because it is thermally stable up to high temperatures. In addition, Pr ions in both Pr123 and Pr124 become antiferromagnetic ordered at the antiferromagnetic transition temperature $T_N = 17$ K.^{5,6}

The compound $\text{Pr}_2\text{Ba}_4\text{Cu}_7\text{O}_{15-\delta}$ (Pr247) is an intermediate between Pr123 and Pr124. In this compound, CuO single-chain and double-chain blocks are alternately stacked along the *c*-axis^{7,8} (see Fig.1). The physical properties of the metallic CuO double chains can be examined by controlling the oxygen content along the semiconducting CuO single chains. Anisotropic resistivity

measurements of single-crystal Pr124 have revealed that metallic transport arises by the conduction along the CuO double chains.⁹ In oxygen removed polycrystalline $\text{Pr}_2\text{Ba}_4\text{Cu}_7\text{O}_{15-\delta}$, superconductivity appears at an onset temperature T_c^{on} of ~ 15 K.¹⁰ Hall coefficient measurements of superconducting Pr247 with $T_c^{\text{on}} = 15$ K have revealed that at intermediate temperatures below 120 K, the main carriers change from holes to electrons, as the temperature decreases. Accordingly, this compound is an electron-doped superconductor.¹¹ In our previous study, we examined the effect of magnetic fields on the superconducting phase of Pr247.¹² Despite of the resistive drop associated with the superconducting transition, we found that the diamagnetic signal was strongly suppressed as expected in the 1D superconductivity of CuO double chains. We also reported the temperature dependence of the Hall coefficient in superconducting Pr247 with a higher $T_c^{\text{on}} \sim 27$ K.¹³ Our findings indicated that the superconducting transition temperature increased because the density of doped electron carriers became denser under the reduction treatment, consistent with a theoretical prediction.¹⁴

In this paper, we demonstrate the thermodynamic properties of the electron-doped metallic double-chain compound $\text{Pr}_2\text{Ba}_4\text{Cu}_7\text{O}_{15-\delta}$, which has a higher T_c^{on} (26.5 K), under different magnetic fields. Figure 1 displays the typical crystal structure of $\text{Pr}_2\text{Ba}_4\text{Cu}_7\text{O}_{15-\delta}$, in which the CuO metallic double chains and semiconducting single chains are alternately stacked along the *c*-axis. Section II outlines the experimental methods, and Sec. III presents the magneto-transport and magneto-thermodynamic properties of polycrystalline Pr247 samples. Along with the magneto-transport data, we report the temperature dependences of the specific heats in the

as-sintered and reduced Pr247. These results are discussed in terms of a three-level system (quasi triplet), in which the ground-state of the Pr^{3+} ions is split by the crystal field effect. The final section is devoted to a summary.

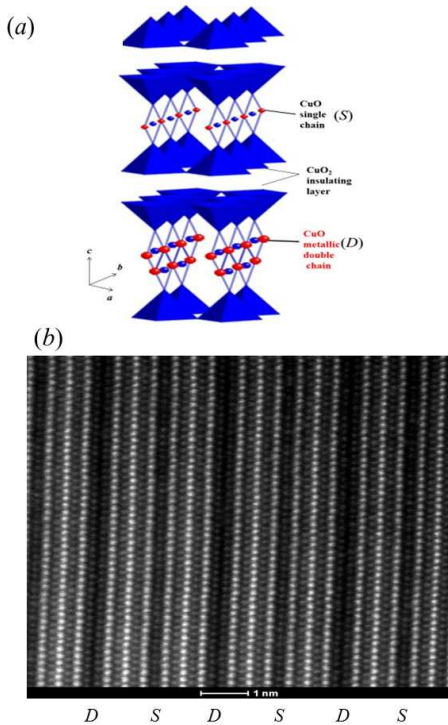


Fig. 1: (color online) (a) Typical crystal structure of $\text{Pr}_2\text{Ba}_4\text{Cu}_7\text{O}_{15-\delta}$ compound. Blocks of CuO single chains (denoted S) and CuO double chains (D) are alternately stacked along c -axis. (b) TEM image of superconducting $\text{Pr}_2\text{Ba}_4\text{Cu}_7\text{O}_{15-\delta}$ compound with a superconducting onset temperature T_c^{on} of 26.5 K.

II. EXPERIMENT

Polycrystalline samples of $\text{Pr}_2\text{Ba}_4\text{Cu}_7\text{O}_{15-\delta}$ (Pr247) were synthesized by the citrate pyrolysis method.¹⁵ After several annealing processes, the resulting precursors were pressed into a pellet and calcined at 875–887 °C for an extended period over 120–180 h under ambient oxygen pressure. The oxygen in the as-sintered sample was removed by reduction treatment in a vacuum at 500 °C for 48 h, yielding a superconducting material. Typical dimensions of the pelletized rectangular sample were $9.9 \times 2.4 \times 1.7 \text{ mm}^3$. The Pr247 sample with $T_c^{\text{on}} = 26.5$ K was observed by high-resolution transmission electron microscopy using a JEOL3010 microscope operated at

300 kV at Tohoku University. The local crystal structure was analyzed from images obtained by the high-angle annular dark-field scanning transmission electron microscope method.¹⁶ The oxygen deficiency in the sample with $T_c^{\text{on}} = 26.5$ K prepared by the citrate method was estimated to be $\delta = 0.56$ from gravimetric analysis. As a function of the oxygen deficiency, the T_c^{on} rises rapidly at $\delta \gtrsim 0.2$, then monotonically increases with increasing δ , and finally saturates around 26–27 K at $\delta \gtrsim 0.6$.¹⁷ Accordingly, the carriers in the present sample are concentrated around the optimally doped region.

The electric resistivity in zero magnetic field was measured by the dc four-terminal method. The magneto-transport up to 9 T was measured by the ac four-probe method using a physical property measuring system (PPMS, Quantum Design), increasing the zero-field-cooling (ZFC) temperatures from 2 K to 40 K. The high field resistivity (up to 14 T) was measured in a superconducting magnet at the High Field Laboratory for Superconducting Materials, Institute for Materials Research, Tohoku University. The electric current I was applied longitudinally to the sample; consequently, the applied magnetic field H was transverse to the sample (because $H \perp I$). The specific heats in the ZFC mode were measured to be between 2 K and 40 K by the PPMS. For comparison, the temperature dependence of the specific heat of the superconducting $\text{Y}_2\text{Ba}_4\text{Cu}_7\text{O}_{15-\delta}$ (Y247) compound prepared by the high-pressure oxygen method⁸ was separately measured in zero field at NIMS.

The dc magnetization was performed under ZFC in a commercial superconducting quantum interference device magnetometer (Quantum Design, MPMS). Magnetic fields of 0.002 T, 0.01 T, 1 T, 3 T, and 5 T were applied.

III. RESULTS AND DISCUSSION

Figure 1 shows the typical crystal structure and a TEM image of the superconducting $\text{Pr}_2\text{Ba}_4\text{Cu}_7\text{O}_{15-\delta}$ compound with $T_c^{\text{on}} = 26.5$ K. S and D denote CuO single-chain and double-chain blocks, respectively. We observe a regular stacking structure of $\{-D-S-D-S-D\}$. In the x-ray diffraction pattern of polycrystalline $\text{Pr}_2\text{Ba}_4\text{Cu}_7\text{O}_{15-\delta}$ synthesized by the citrate pyrolysis method, a clear peak corresponding to the Miller index (004) of Pr247 was observed, but peaks of Pr123 or Pr124 phases were absent (data not shown).¹²

Figure 2 plots the temperature dependences of the magnetic susceptibilities of the non-superconducting and superconducting samples under various magnetic fields (up to 5 T). In the as-sintered sample, a typical anomaly in χ occurs near 17 K. This anomaly is associated with an antiferromagnetic transition of the Pr sublattice, as previously reported in Pr123 and Pr124 systems.^{5,6} On the contrary, the 48-h-reduced sample becomes superconductive below $T_c^{\text{on}} = 26.5$ K. The superconducting volume fraction f was estimated from the magnetic data taken

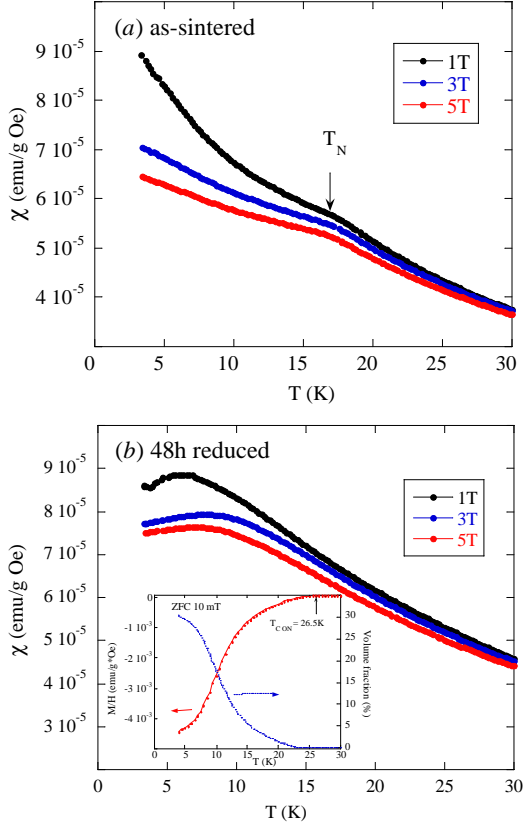


Fig. 2: (color online) Low-temperature dependences of magnetic susceptibilities χ of $\text{Pr}_2\text{Ba}_4\text{Cu}_7\text{O}_{15-\delta}$ compounds under various magnetic fields (1 T, 3 T, and 5 T). (a) Non-superconducting as-sintered sample and (b) superconducting 48-h-reduced sample with $T_{c,on} = 26.5$ K. Inset plots are magnetic data recorded at 10 mT, from which we estimated $T_c^{on} = 26.5$ K. Superconducting volume fractions estimated from present data are also plotted (right vertical axis in inset).

at 10 mT by $f = \chi \cdot \rho / 4\pi \times 100$, where χ and ρ denote the magnetic susceptibility per unit weight and the sample density (5.3 g/cm^3), respectively. As displayed in the inset of Fig.2 (b), the volume fraction reaches $\sim 30\%$ at 4 K, indicating bulk superconductivity.

However, under high fields, the magnetic data of the superconducting sample monotonically increases as the temperature decreases to below 17 K and saturate at low temperatures. This trend reflects the ferromagnetic character of the sample. As highlighted in our previous paper,¹² the diamagnetic signal is suppressed despite the resistive drop associated with the superconducting transition. This observation is closely related to the 1D superconductivity of CuO double-chains. In contrast to the positive magnetization data at higher field, the resistivity data of the 48-h-reduced sample substantially drop as the transport currents becomes superconducting (see Fig.3(b)). The clear difference in the magnetic behav-

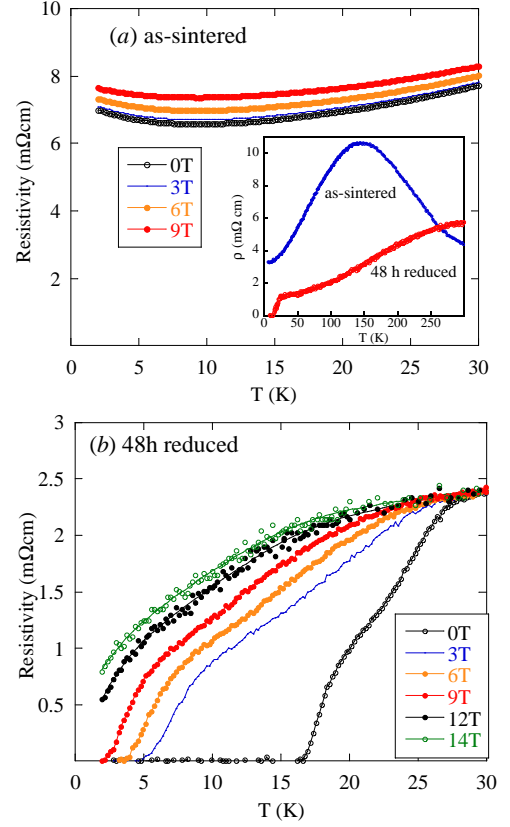


Fig. 3: (color online) Low-temperature dependences of electric resistivities of $\text{Pr}_2\text{Ba}_4\text{Cu}_7\text{O}_{15-\delta}$ compounds measured under various magnetic fields. (a) As-sintered non-superconducting sample, measured at 0 T, 3 T, 6 T, and 9 T, and (b) 48-h-reduced superconducting sample with $T_{c,on} = 26.5$ K, measured at 0 T, 3 T, 6 T, 9 T, 12 T, and 14 T. For comparison, inset plots resistivity data of both samples versus T (between 2 K and 300 K).

ior between the as-sintered and reduced samples reflects the different magnetic interactions among the Pr magnetic ions. The Pr atoms in Pr_{124} , are well separated, so their antiferromagnetic ordering is not dominated by the superexchange interaction. Instead, we consider that the antiferromagnetic coupling of the Pr sublattice occurs due to the Rudermann-Kittel-Kasuya-Yoshida (RKKY) interaction and is mediated by itinerant carriers as noted by Xu et al.¹⁹ In Pr_{247} , the vacuum reduction treatment varies the distance between the Pr ions, and the ferromagnetic property of the reduced sample occurs through the RKKY interaction.

From the magnetic susceptibility measurements over a wide range of temperatures range (20-200 K), we estimate the effective magnetic moment μ_{eff} of the Pr ions by the Curie-Weiss law. Performing the calculation, we obtained that $\mu_{\text{eff}} = 3.02$ and $3.26 \mu_B$ for the non-superconducting and superconducting samples, re-

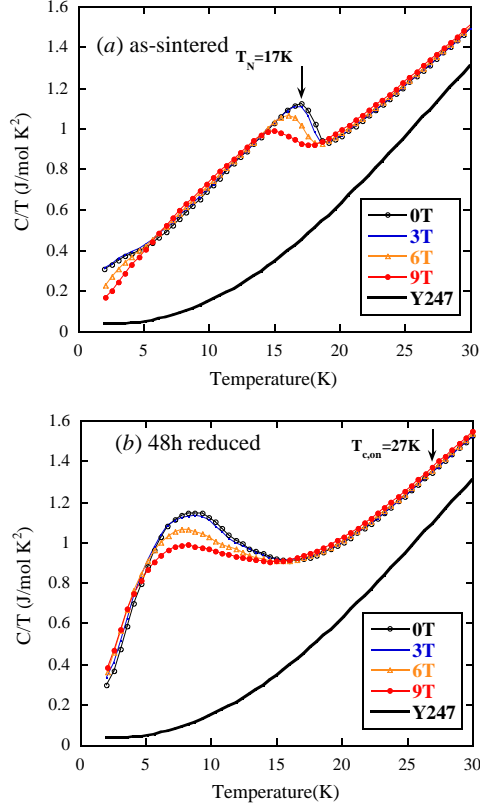


Fig. 4: (color online) Temperature dependences of specific heats of $\text{Pr}_2\text{Ba}_4\text{Cu}_7\text{O}_{15-\delta}$ compounds under various magnetic fields (up to 9 T). (a) The non-superconducting as-sintered sample and (b) the superconducting 48-h-reduced sample with $T_{c,on} = 26.5$ K. For comparison, zero-field specific heat data of superconducting $\text{Y}_2\text{Ba}_4\text{Cu}_7\text{O}_{15-\delta}$ (Y247) prepared in high-pressure oxygen are also plotted.

spectively. These values are almost consistent with the effective moment of Pr124 ($\mu_{\text{eff}} = 3.11\mu_B$).⁶ In particular, the μ_{eff} of the superconducting sample is close to that of Pr^{3+} ($3.54\mu_B$).

The magnetoresistance of the as-sintered and 48-h-reduced samples also differ at high temperatures (above $T_c^{\text{on}} = 26.5$ K). In our next paper, concerning the effects of external pressure on the magneto-transport of superconducting and non-superconducting Pr247, we will link this difference to the electronic phase diagram of the 1D zigzag CuO chain model.

Figure 4 plots the temperature dependences of the specific heats C/T of the non-superconducting and superconducting Pr247 compounds under several magnetic fields (up to 9 T). The C/T of the non-superconducting as-sintered sample exhibits a λ -like enhancement associated with the antiferromagnetic transition of Pr ions, as previously reported in non-superconducting Pr123 and Pr124 systems.^{6,18} As the external magnetic field in-

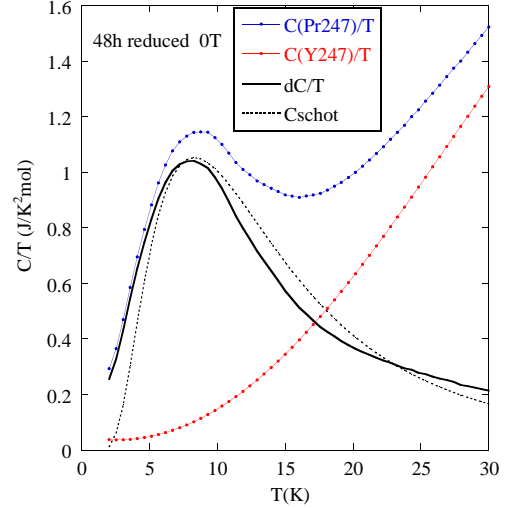


Fig. 5: (color online) Temperature dependences of specific heat differences $\Delta C/T$ observed in Pr247 and Y247 (C_{Pr247}/T and C_{Y247}/T , respectively). Dashed curves are calculated Schottky heat anomalies due to crystal field splitting of Pr^{3+} . Parameters under zero field were fitted as $E_1 = 23.2\text{ K}$ and $E_2 = 46.4\text{ K}$.

creases, this sharp increase is suppressed and peaks at lower temperatures. At 9 T, the thermodynamic peak is considerably depressed and is located around 15 K. At low temperatures (below 5 K), the specific heat also exhibits a strong field dependence, for reasons which have not yet been clarified. On the other hand, the C/T of the superconducting sample is not enhanced at temperatures above 15 K, regardless of the applied magnetic field. The absence of λ -like enhancement in reduced Pr247 appears to be consistent with the corresponding magnetic behavior, which shows no clear AFM transition. At temperatures below 15 K, the C/T of the superconducting sample shows a broad peak around 8.5 K. This broad anomaly is strongly suppressed under a magnetic field. For comparison, Fig.4 also plots the temperature dependence of the specific heat of superconducting Y247 in the absence of magnetic field, which was prepared by the high pressure oxygen method. Oxygen removed $\text{Y}_2\text{Ba}_4\text{Cu}_7\text{O}_{14}$, with no superconductivity down to 2 K, exhibits a C/T magnitude and temperature dependence

similar to those of the superconductor Y247.²⁰ Accordingly, because Y247 and Pr247 share the same crystal structure, we roughly assumed the low-temperature specific heat of superconducting Y247 to be the lattice component of the Pr247 sample. We further assumed that the low-temperature dependences of the electronic components of both Y247 and Pr247 were significantly smaller than those of the lattice parts.

Figure 5 plots the specific heat differences dC/T between the superconducting Pr247 and Y247 data, (C_{Pr247}/T and C_{Y247}/T , respectively) versus temperature. Comparing our results with the previous data obtained using Pr-based 123,²¹ it is evident that the low-temperature specific heat data of $\text{PrBa}_2\text{Cu}_3\text{O}_7$ and $\text{PrBa}_2\text{Cu}_3\text{O}_6$ follow temperature trends, similar to those of as-sintered and vacuum-reduced Pr247, respectively. The common features include the λ -like enhancement in the former compounds and the broad C/T maximum in the latter. To analyze the low-temperature peak in the specific heat trends of $\text{PrBa}_2\text{Cu}_3\text{O}_6$, Hilscher et al²¹ introduced a Schottky type specific heat contributed by a thermal population of electrons. In this study, we followed Hilscher's approach to understand the broad maximum in the C/T of the corresponding superconducting Pr247.²² In the Pr123 system, the crystal field ground state of the Pr ion is a quartet and is separated by several tens of meV from the group of remaining crystal field levels.^{21,23} Accordingly, we assumed that at temperatures below 30 K, the energy levels of the Pr ion are split into three by the crystal field effect.

Assuming that for three energy levels E_i ($i = 0, 1, \text{ and } 2$) $E_0 = 0$ K and $E_1 < E_2$, we then get a partition function for the three energy level system, $Z = 1 + e^{-\beta E_1} + e^{-\beta E_2}$ ($\beta = 1/kT$). Substituting the above formula into a general expression for a specific heat, $C = \frac{1}{kT^2} \frac{d^2 \log Z}{d\beta^2}$, a Schottky-type specific heat with three energy levels is given by

$$C_{\text{Sch}} = k_B \frac{x^2 e^{-x} + y^2 e^{-y} + (x-y)^2 e^{-x-y}}{(e^{-x} + e^{-y} + 1)^2}$$

where $x = E_1/T$ and $y = E_2/T$ denote the temperature reduced energy levels.

As shown in Fig.5, the zero field data below 30 K are roughly fitted by the Schottky expression with $E_1 = 23.2K$ and $E_2 = 46.4K$. The energy levels fitted to the curves of the superconducting Pr247 compound are similar to the experimental and calculated crystal field levels of the 3H_4 multiplet in $\text{PrBa}_2\text{Cu}_3\text{O}_6$, which has orthorhombic crystal field parameters. For example, as pre-

dicted from inelastic neutron scattering measurements of $\text{PrBa}_2\text{Cu}_3\text{O}_6$, the crystal field splitting of this compound is $E_1 = 19.7K$ and $E_2 = 39.4K$.²¹ The low-temperature peak in the specific heat of the oxygen-removed superconducting sample is reasonably described by the Schottky anomaly (see Fig.5). The small discrepancy between the calculated curve and the experiment data is probably attributed to magnetic interactions among the Pr ions. The reduced superconducting sample shows no obvious anomaly associated with the superconducting transition, inconsistent with the experimentally observed resistive drop and diamagnetic signal as the temperature decreases. As shown in the inset of Fig.2, the superconducting volume fraction is several percent around 15 K, and rapidly increases as the temperature falls below 10 K. Thus, we infer that the superconducting anomaly of metallic CuO double chains is masked by the Schottky like broad enhancement in C/T caused by the crystal field effect of the Pr ions.

IV. SUMMARY

We demonstrated the thermodynamic properties of superconducting and non-superconducting $\text{Pr}_2\text{Ba}_4\text{Cu}_7\text{O}_{15-\delta}$ compounds with metallic CuO double chains. For this purpose, we measured the specific heats of the polycrystalline samples at low temperatures under varying magnetic fields (up to 9 T). The specific heat of the as-sintered non-superconducting sample displayed the λ -like enhancement near the antiferromagnetic transition temperature $T_N = 17$ K. This anomaly around the superconducting transition was absent in the reduced superconducting sample for reasons related to the small superconducting volume fraction at temperatures above 15 K. As the temperature decreased below 15 K, the C/T of the superconducting sample broadly peaked around 8.5 K. This Schottky-like broad maximum was attributed to low-lying quasi-triplet splitting of Pr^{3+} ions under the crystal field effect.

Acknowledgments

The authors are grateful for M. Nakamura for his assistance in PPMS experiments at Center for Regional Collaboration in Research and Education, Iwate University.

* Electronic address: matsukawa@iwate-u.ac.jp

¹ L. Soderholm, K. Zhang, D. G. Hinks, M. A. Beno, J. D. Jorgensen, C. U. Segre, I. K. Schuller, Nature 328 (1987) 604.

² S. Horii, Y. Yamada, H. Ikuta, N. Yamada, Y. Kodama,

S. Katano, Y. Funahashi, S. Morii, A. Matsushita, T. Matsumoto, I. Hirabayashi, and U. Mizutani, Physica C 302 (1998) 10.

³ R. Fehrenbacher and T. M. Rice, Phys. Rev. Lett. 70 (1993) 3471.

- ⁴ T. Mizokawa, C. Kim, Z. -X. Shen, A. Ino, T. Yoshida, A. Fujimori, M. Goto, H. Eisaki, S. Uchida, M. Tagami, K. Yoshida, A. I. Rykov, Y. Siohara, K. Tomimoto, S. Tajima, Yuh Yamada, S. Horii, N. Yamada, Yasuji Yamada, and I. Hirabayashi, *Phys. Rev. Lett.* 85 (2000) 4779.
- ⁵ W.-H. Li, J. W. Lynn, S. Skanthankumar, T. W. Clinton, A. Kebede, C. S. Jee, J. E. Crow, and T. Mihalisin, *Phys. Rev. B* 40 (1989) 5300.
- ⁶ H. D. Yang, J.-Y. Lin, S. S. Weng, C. W. Lin, H. L. Tsay, Y. C. Chen, T. H. J. Meen, T. I. Hsu, and H. C. Ku, *Phys. Rev. B* 56 (1997) 14180.
- ⁷ P. Bordet, C. Chaillout, J. Chenavas, J. L. Hodeau, M. Marezio, J. Karpinski, and E. Kaldis, *Nature* 334 (1988) 596.
- ⁸ Y. Yamada, S. Horii, N. Yamada, Z. Guo, Y. Kodama, K. Kawamoto, U. Mizutani, and I. Hirabayashi, *Physica C* 231(1994)131.
- ⁹ S. Horii, U. Mizutani, H. Ikuta, Y. Yamada, J. H. Ye, A. Matsushita, N. E. Hussey, H. Takagi, and I. Hirabayashi, *Phys. Rev. B* 61 (2000) 6327.
- ¹⁰ M. Matsukawa, Y. Yamada, M. Chiba, H. Ogasawara, T. Shibata, A. Matsushita, and Y. Takano, *Physica C* 411 (2004) 101.
- ¹¹ A. Matsushita, K. Fukuda, Y. Yamada, F. Ishikawa, S. Sekiya, M. Hedo, and T. Naka, *Science and Technology of Advanced Materials* 8 (2007) 477.
- ¹² T. Chiba, M. Matsukawa, J. Tada, S. Kobayashi, M. Hagiwara, T. Miyazaki, K. Sano, T. Sasaki, and J. Echigoya, *J. Phys. Soc. Jpn.*, 82 (2013) 074706.
- ¹³ J. Tada, M. Matsukawa, T. Konno, S. Kobayashi, M. Hagiwara, T. Miyazaki, K. Sano, and A. Matsushita, *J. Phys. Soc. Jpn.*, 82 (2013) 105003.
- ¹⁴ K. Sano, Y. Ono, and Y. Yamada, *J. Phys. Soc. Jpn.*, 74 (2005) 2885.
- ¹⁵ M. Hagiwara, T. Shima, T. Sugano, K. Koyama, and M. Matsuura, *Physica C* 445-448 (2006) 111.
- ¹⁶ S. J. Pennycook and D. E. Jesson, *Phys. Rev. Lett.* 64 (1990) 938.
- ¹⁷ M. Hagiwara, S. Tanaka, T. Shima, K. Gotoh, S. Kanda, T. Saito, and K. Koyama, *Physica C* 468 (2008) 1217.
- ¹⁸ A. Kebede, C. S. Jee, J. Schwegler, J. E. Crow, T. Mihalisin, G. H. Myer, R. E. Salomon, P. Schlottmann, M. V. Kuric, S. H. Bloom, and R. P. Guertin, *Phys. Rev. B* 40 (1989) 4453.
- ¹⁹ X. Xu, A. Carrington, A. I. Coldea, A. Enayati-Rad, A. Narduzzo, S. Horii, and N. E. Hussey, *Phys. Rev. B* 81 (2010) 224435.
- ²⁰ A. Irizawa, T. Ohmura, T. Shibata, M. Kato, K. Yoshimura, K. Kosuge, Y. Ito, H. Michor, and G. Hilscher, *J. Phys. Soc. Jpn.* 71(2002)574.
- ²¹ G. Hilscher, E. Holland-Moritz, T. Holubar, H. -D. Jostarndt, V. Nekvasil, G. Schaudy, U. Walter, and G. Fillion, *Phys. Rev. B* 49 (1994) 535.
- ²² C. Kittel, *Introduction to the Solid State physics* 5th edn (New York: Wiley) 1976.
- ²³ L. Soderholm, C. -K. Loong, G. L. Goodman, and B. D. Dabrowski, *Phys. Rev. B* 43 (1991) 7923.